ChemPubSoc Europe

DOI: 10.1002/chem.201701365

CHEMISTRY A European Journal Full Paper

Fluorescent Probes |*Hot Paper*|

Rational Development of Near-Infrared Fluorophores with Large Stokes Shifts, Bright One-Photon, and Two-Photon Emissions for Bioimaging and Biosensing Applications

Liyi Zhou,*[a, b] Qianqian Wang,[b] Yi Tan,[c] Matthew J. Lang,[d, e] Hongyan Sun,*[c, f] and Xiaogang Liu*[d]

Abstract: Fluorophores with near-infrared emissions play a crucial role in numerous bioimaging and biosensing applications, owing to their deep penetration depths, low auto-fluorescence, and minimal tissue damages. Herein, the rational development of a new class of near-infrared fluorophores with bright one-photon and two-photon emissions at ≈740 nm, large Stokes shifts (≈80 nm), significant two-photon action absorption cross-section (≈185 GM at 820 nm), excellent water solubility, outstanding photostability, and low toxicity is reported. Their biological applications in mitochondrial labelling, deep tissue imaging, and H_2S detection in live cells and mice are also demonstrated. In addition, a rational design strategy for enlarging the Stokes shifts and enhancing two-photon emissions of these fluorophores is presented. These fluorophores will serve as a useful platform for developing novel imaging and sensing agents, and the design methodologies will inspire the molecular engineering of abundant high-performance near-infrared fluorophores.

Introduction

Bright near-infrared (NIR) fluorophores are indispensable in numerous bioimaging and biosensing applications. Their long emission wavelengths (650–900 nm) permit deeper tissue penetrations (up to ≈1 cm), less auto-fluorescence, and lower tissue damage in comparison to visible light.[1] Currently, the most widely used NIR dyes are cyanine derivatives.[2] Most cyanine dyes, however, are vulnerable to molecular aggregation and photobleaching.[3] In recent years, considerable research efforts have led to the remarkable development of NIR Changsha dyes,[4] Keio-BODIPY dyes,[5] and Si-Rhodamines.[6] Unfortunately, most of these NIR fluorophores exhibit small Stokes shifts (<30 nm), rendering them susceptible to inner-filter effect (the reabsorption of fluorescence).

Developing NIR fluorophores with bright two-photon (TP) emissions is an even more challenging task, due to the complexity of the TP absorption process. To date, many existing TP fluorophores exhibit visible emissions (400–650 nm).[7] Such fluorophores are typically acedan and naphthalene derivatives, with TP action cross-sections ($\sigma\varphi$, the product of TP absorption cross-section and quantum yield) of <120 Goeppert-Mayer (GM).[8] Moving towards longer wavelengths, Bewersdorf and co-workers demonstrated that several red and far-red (carbon-/silicon-) rhodamine derivatives exhibit large $\sigma\varphi$ values (> 100 GM) in the second absorption band (SAB; $S_0 \rightarrow S_n$ transition; $n > 1$) of two-photon absorption (2PA) spectra.[9] In the NIR region, Fu et al. showed that a large SAB is present in the 2PA spectra of cyanine dyes.[10] Two-photon near-infrared (TP-NIR) fluorescent probes have also been constructed based on 4-(dicyanomethylene)-styryl-4*H*-pyran dyes ($\sigma\varphi < 50$ GM).[11] Unfortunately, existing TP-NIR dyes suffer from either poor photostability or low quantum yields. More fundamentally, detailed design guidelines are still lacking to assist the systematic development of TP-NIR fluorophores with improved brightness.

[a] *Prof. Dr. L. Zhou*
College of Food Science and Technology,
Central South University of Forestry and Technology,
Changsha, Hunan 410004 (P. R. China)
E-mail: zhouly0817@163.com

[b] *Prof. Dr. L. Zhou, Q. Wang*
State Key Laboratory of Chemo/Biosensing and Chemometrics,
Hunan University, Changsha, Hunan 410082 (P. R. China)

[c] *Y. Tan, Prof. Dr. H. Sun*
Department of Biology and Chemistry,
City University of Hong Kong,
83 Tat Chee Avenue, Kowloon, Hong Kong (P. R. China)
E-mail: hongysun@cityu.edu.hk

[d] *Prof. Dr. M. J. Lang, Dr. X. Liu*
Singapore-MIT Alliance for Research and Technology (SMART),
1 CREATE Way, Singapore 138602 (Singapore)
E-mail: xiaogang@smart.mit.edu

[e] *Prof. Dr. M. J. Lang*
Department of Chemical and Biomolecular Engineering and
Department of Molecular Physiology and Biophysics,
Vanderbilt University, Nashville, TN 37235 (USA)

[f] *Prof. Dr. H. Sun*
Biotechnology and Health Centre,
Shenzhen Research Institute of City University of Hong Kong,
Shenzhen 518057 (P. R. China)

Supporting information for this article can be found under: https://doi.org/10.1002/chem.201701365.

In this paper, we have proposed and validated rational design strategies to enlarge the Stokes shifts and enhance 2PA of fluorophores. Accordingly, our newly developed fluorophores **1** and **2** demonstrate significant $\sigma\varphi$ values ($\approx$185 GM at 820 nm), along with bright NIR emission ($\approx$740 nm), large Stokes shift ($\approx$80 nm), excellent water solubility, outstanding photostability, low toxicity, and facile synthesis (Figure 1 a). We also demonstrate their biological applications in deep tissue imaging and H_2S detection in live cells and mice.

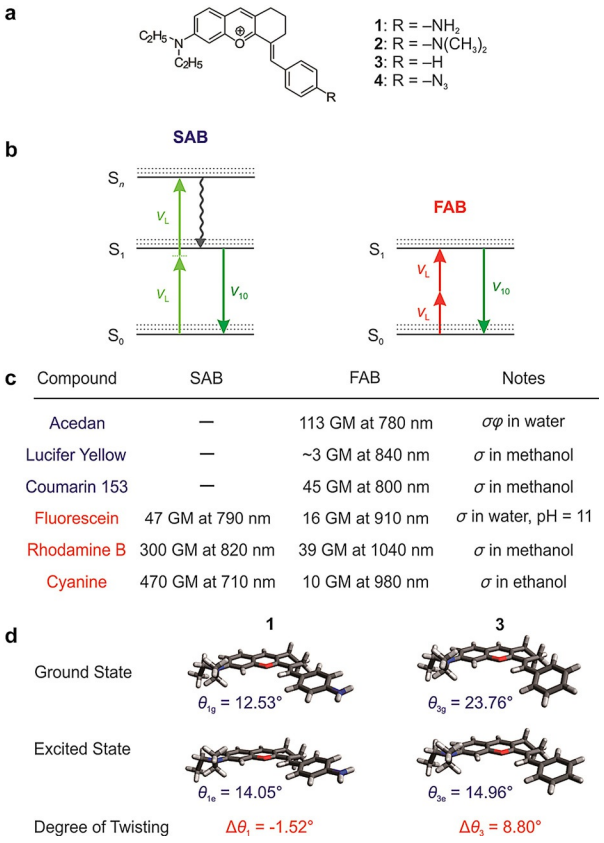

Figure 1. (a) Molecular structures of **1**–**4**. (b) Jablonski diagram of the second absorption band (SAB) and first absorption band (FAB) transitions during a two-photon absorption/emission process. (c) Two-photon absorption cross sections (σ) or two-photon action cross sections ($\sigma\varphi$) in FAB and SAB of the two-photon absorption spectra of representative high-polarity (highlighted in blue) and low-polarity dyes (highlighted in red), as reported in literature.[6,14,17] (d) Optimized molecular geometries of **1** and **3** in the ground (S_0) and the first excited singlet (S_1) states in water, using B3LYP/6–31+G(d,p); θ represents the dihedral angle between the phenyl ring and the fluorophore scaffold of **1** and **3**.

Results and Discussion

Molecular design strategies

To ensure bright two-photon emissions, our first design strategy leverages SAB ($S_0 \rightarrow S_n$ transition; $n > 1$) instead of the first absorption band (FAB; $S_0 \rightarrow S_1$ transition) for exciting NIR fluorophores. To this end, Drobizhev et al. have shown that SAB "amplifies" 2PA via the resonance enhancement effect in fluorescent proteins.[12] This enhancement effect becomes significant as laser excitation wavelength gets close to fluorophore emission wavelength (Figure 1 b; Supporting Information 1). Consequently, SAB is often stronger than FAB in the 2PA of fluorescent proteins.

We further performed a comprehensive literature search on 2PA data of approximately 100 fluorophores from different chemical families and compared the resonance enhancement effect in both low-polarity and high-polarity dyes.[8a,10,13] Our analysis on 2PA data reveals an interesting trend: for highly polar fluorophores (such as coumarin, naphthalimide, and acedan dyes), a large FAB is present in the 2PA spectra (Figure 1 c). As the fluorophore polarity deceases, the strength of SAB increases. For example, in the 2PA spectra of fluorescein, rhodamine, and cyanine dyes, SAB particularly strengthens, up to 47 times larger than FAB (Figure 1 c). The more significant resonance enhancement effect in these low-polarity dyes is largely related to their higher molar extinction coefficients than those of high-polarity dyes (see Supporting Information 1 for a detailed discussion).

Our second design strategy concerns the Stokes shift of organic fluorophores. Interestingly, our previous research shows that incorporating a rotary substituent significantly increases the geometry relaxation of a fluorophore in the excited state, thereby enlarging its Stokes shift.[14] Although considerable rotations quench fluorescence (such as in molecular rotors), we also find that controlling substituent rotations to a small degree could still preserve high quantum yields.[15]

Inspired by these discoveries, we turned our attention to **3**, a low-polarity fluorophore (Figure 1 a).[16] Compound **3** has longer absorption wavelengths than many conventional fluorophores (such as coumarin, naphthalimide, acedan, BODIPY and rhodamine derivatives). Synthesis of **3** is facile, and the availability of an amino group in this compound makes further chemical substitution and functionalization straightforward. More importantly, our quantum chemical calculations show that the TP absorption cross-section (σ) of **3** is about 4–20 times larger than those of popular naphthalimide, acedan, rhodamine, and Nile Red dyes (see the Supporting Information 2).

Although **3** demonstrates a large TP absorption cross-section, its quantum yield is close to zero. Our calculations show that the low quantum yield of **3** is primarily related to the rotation of its phenyl ring upon photoexcitation (Figure 1 d; Supporting Information 2). Due to steric hindrance, this phenyl ring exhibits a dihedral angle of 23.76° with respect to the fluorophore scaffold of **3** in the ground state. This dihedral angle reduces to 14.96° upon photoexcitation. Such a significant rotation by 8.80° markedly diminishes the quantum yield of **3**. Nevertheless, our calculations also show that by attaching an electron-donating group (i.e., -NH_2) at the *para*-position of the phenyl group, the dihedral angle drops to 12.53° in the ground state of **1**, and the resulted aminophenyl ring experiences a small rotation by only 1.52° upon photoexcitation. Consequently, we predict that **1** and **2** have good quantum yields. Furthermore, the more planar molecular structures of **1** and **2** will bathochromically shift their absorption and emission spectra compared to that of more twisted **3** (λ_{abs} = 560 nm); and

the slight rotation of the aminophenyl rings upon photoexcitation enlarges the Stokes shifts of **1** and **2**.[14,15]

Synthesis and Characterizations

Experimental data are in good agreement with our design analysis (Figure 2a; see the Supporting Information 3). We synthesized compounds **1** and **2**, via a two-step reaction with good yields (70–95%). These compounds carry different groups [-NH_2 and -$N(CH_3)_2$] at the *para*-position of the phenyl ring in **3** (Figure 1a). As expected, **1** and **2** exhibit one-photon peak absorption (≈660 nm) and emission (≈740 nm) in the NIR optical window (Figure 2b and c). They possess high quantum yields (φ = 12.7% for **1** and 11.3% for **2** in pH 7.4 PBS), and large Stokes shifts (75 and 82 nm for **1** and **2**, respectively).

During 2PA characterization, we find a strong second absorption band peaked at 820 nm in both **1** and **2** (Figure 2d). Interestingly, this TP excitation wavelength falls into the optical window and can be excited in standard TP microscopes equipped with tunable Ti:Sapphire lasers. Moreover, the TP action cross-sections ($\sigma\varphi$) values of **1** and **2** are up to 180 and 190 GM, respectively. Such large $\sigma\varphi$ values are among the highest in NIR fluorophores.

We also investigated the effect of pH on the optical properties of **1** and **2** (Figure 2e). Their emission intensities remain relatively stable between pH 4 and 6, but exhibit a ≈30% drop at pH 8. This drop can be recovered by reducing pH. We speculate that this reversible pH modulation of emission intensity in **1** and **2** is related to the break of oxygen bridge bonds in strongly basic conditions. Nevertheless, absolute fluorescence intensities of **1** and **2** remain high between pH 4 and 8 (φ ≈12% at pH 7.4).

These compounds also demonstrate excellent photostability. When subjected to 30 min of irradiation with a 100 W mercury lamp, a control fluorophore, namely MitoTracker Green (**MG**), exhibits ≈90% decrease in its fluorescence intensity. In contrast, **1** experiences < 5% drop (Figure 2f).

We choose **1** as a model compound to further evaluate its biocompatibility. MTT assay experiments using HeLa cells show that **1** possesses low cytotoxicity over a concentration range from 0 to 10 μM (≈90% viability after 24 hours of incubation; Figure 2g). Fluorophore **1** also demonstrates good water solubility, mainly because of its ionic nature.

a

Dye	λ_{abs} [nm]	ε [M^{-1} cm^{-1}]	λ_{em} [nm]	$\Delta\lambda$ [nm]	$\Delta\nu$ [cm^{-1}]
1	650	151,205	725	75	1,592
2	668	154,510	750	82	1,637

Dye	φ	$\lambda_{2PA,exc}$ [nm]	σ [GM]	$\sigma\varphi$ [GM]
1	0.127	820	1,417	180
2	0.113	820	1,681	190

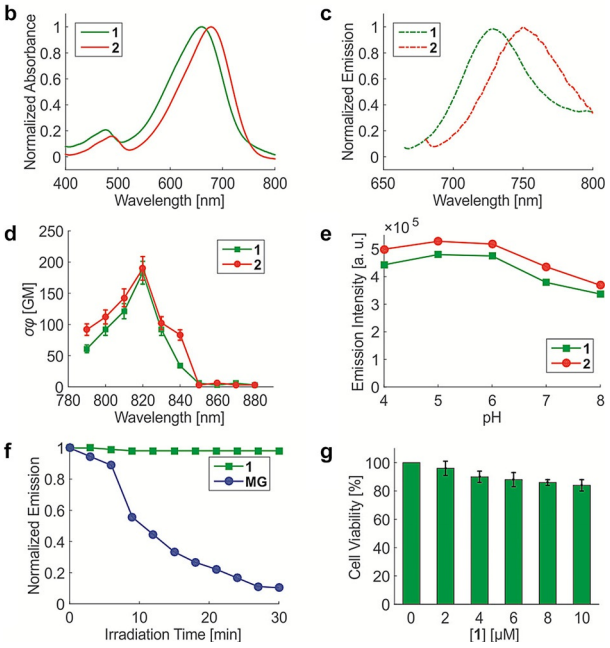

Figure 2. (a) Experimental spectroscopic data for **1** and **2** in 10 mM PBS (pH 7.4) with 0.5% ethanol. λ_{abs}, peak UV/Vis absorption wavelength; ε, molar extinction coefficient; λ_{em}, peak emission wavelength; $\Delta\lambda$ and $\Delta\nu$, the Stokes shift; φ, quantum yield; $\lambda_{2PA,exc}$, peak two-photon excitation wavelength; σ, two-photon absorption cross section; $\sigma\varphi$, two-photon action cross section. (b) One-photon UV/Vis absorption, (c) emission, and (d) two-photon action absorption cross-section spectra of **1** and **2** in 10 mM PBS (pH 7.4) with 0.5% ethanol. (e) Effect of pH on the fluorescence intensities of **1** and **2**, excited at 650 and 668 nm, respectively. (f) Photostability of **1** and **MG** under 30 min irradiation of a 100 W mercury lamp in vitro. (g) Viabilities of HeLa cells after 24 hours of incubation in 0–10 μM of **1**.

Bioimaging applications

Given the suitability of **1** in bioimaging applications, we firstly performed one-photon bioimaging experiments in labelling mitochondria (Figure 3a; see the Supporting Information 3). Positively charged **1** displays mitochondria-specific staining in

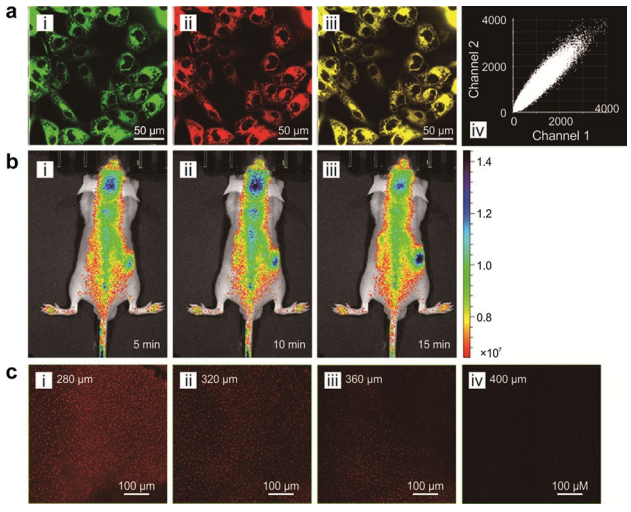

Figure 3. (a) Colocalization images of A375 cells incubated with **1** (1 μM, 30 min) and MitroTracker Green (MG, 1 μM, 30 min): (i) emission from channel 1 (**MG**; λ_{ex} 488 nm; λ_{em} 495–530 nm); (ii) emission from channel 2 (**1**; λ_{ex} 635 nm; λ_{em} 690–740 nm); (iii) overlay of channels 1 and 2; (iv) intensity scatter plot of channels 1 and 2. (b) Fluorescence images (pseudo color) of a nude mouse, (i) 5 (ii) 10, and (iii) 15 min after injecting **1** into the tail veins of the mouse ([**1**] = 20 μM; vol = 20 μL). (c) Two-photon fluorescence imaging of rat liver tissue stained with **1**, at the imaging depth of (i) 280, (ii) 320, (iii) 360, and (iv) 400 μm ([**1**] = 10 μM).

both HeLa and A375 cells. This mitochondrial specificity is confirmed by colocalization experiments using **MG**, a commercially available mitochondrial marker. The overlay coefficient between **1** and **MG** is calculated to be 0.97. Interestingly, while monitoring mitochondria for 60 min under continuous laser excitation, we found the fluorescence of **1** remained bright, whereas that of **MG** considerably dropped (see the Supporting Information 3, Figure S32). These results further corroborate the excellent photostability of **1**, and suggest its long-term tracking applicability.

We also injected **1** into the tail veins of live mice. The injected fluorophores quickly passed through blood–brain barriers and produced strong fluorescence signals within five minutes (Figure 2b). We noticed the accumulation of **1** in mouse kidneys 15 min after the injection.

Inspired by its bright TP emission and long excitation/emission wavelengths, we then studied **1** in deep tissue bioimaging (Figure 2c). We stained a rat liver slice with **1** and took TP excited fluorescence images at different penetration depths. Experimental results show that **1** exhibits improved spatial resolution at the imaging depth between 90 and 400 μm compared to naphthalene derivatives under identical experimental conditions (see the Supporting Information 3, Figure S33). These results suggest the substantial potential of **1** for in vivo TP fluorescence imaging applications.

Biosensing of H_2S

To further prove the utility of our fluorophores, we constructed a turn-on probe **4** for H_2S detection (Figure 1a; Supporting Information 3). H_2S is an important signaling molecule with cytoprotective functions, and an abnormal intracellular H_2S level is related to many critical diseases.[17] In our probe **4**, an electron-withdrawing azide group is introduced for H_2S recognition and fluorescence quenching. The fluorescence turns on in the presence of H_2S, which reacts with the azide group and reduces it to an amino group.[18] Our experiments show that **4** demonstrates low cellular toxicity in HeLa cells (≈90% viability after 24 hours of incubation; Figure 4a). Probe **4** also has good selectivity to H_2S over other biologically relevant analytes (such as $S_2O_3^{2-}$, $S_2O_4^{2-}$, $S_2O_5^{2-}$, SO_3^-, and ascorbic acid; Figure 4b). We also note that **4** shows weak responses towards thiol-containing amino acids including glutathione, cysteine, and homocysteine. In addition, **4** is highly responsive to H_2S (Figure 4c) and the resulted enhancement in fluorescence intensity quantifies H_2S concentration (Figure 4d).

We applied **4** to monitor H_2S in live HeLa cells via TP fluorescence imaging (Figure 4e). After incubating HeLa cells with **4** for 30 min, endogenous thiols activation causes weak fluorescence. For cells pretreated with phorbol myristate acetate (an H_2S inhibitor), incubation with **4** results in negligible fluorescence. In contrast, in HeLa cells pretreated using 50 μM of NaHS (exogenous H_2S source), incubation with **4** for 30 min leads to significantly enhanced fluorescence. Similarly, subsequent experiments in live mice via one-photon bioimaging show that intraperitoneal injection of **4** produces only weak fluorescence signals. However, injecting of **4** followed by NaHS after five minutes triggers intensive fluorescence (Figure S36).

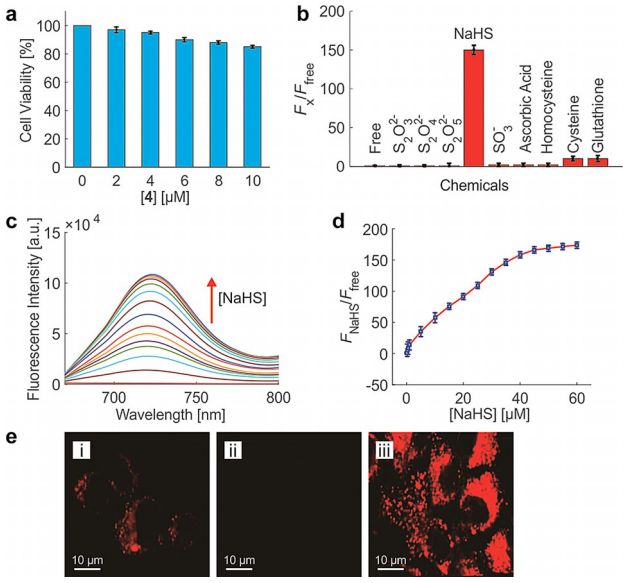

Figure 4. (a) Viabilities of HeLa cells after 24 hours of incubation in 0–10 μM of **4**; (b) Fluorescence intensity enhancement of **4** at 725 nm in the presence of various biologically relevant analytes: (i) free, (ii) 100 equiv of $S_2O_3^{2-}$, (iii) 100 equiv of $S_2O_4^{2-}$, (iv) 100 equiv of $S_2O_5^{2-}$, (v) 50 equiv of NaHS, (vi) 100 equiv of SO_3^-, (vii) 100 equiv of homocysteine, (viii) 100 equiv of ascorbic acid, (ix) 100 equiv of cysteine and (x) 100 equiv of glutathione; λ_{ex} = 650 nm. (c) One-photon fluorescence spectra of **4** (1 μM) in the presence of various concentrations of NaHS (0–150 μM) in PBS buffer (10 mM, pH 7.4). λ_{ex} = 650 nm. (d) Calibration curve of **4** to [NaHS]. The curve was plotted by calculating the intensity ratios of **4** with (F_{NaHS}) and without (F_{free}) the addition of various concentrations of NaHS (after incubation for 10 min). (e) Two-photon microscopy images for H_2S detection in HeLa cells incubated with: (i) 1 μM of **4** for 30 min; (ii) PMA (1 μg mL^{-1}) for 30 min, and then with 1 μM of **4** for another 30 min; (iii) 1 μM of **4** for 30 min and then with 50 μM of NaHS for another 30 min. λ_{ex} = 820 nm.

Conclusion

In conclusion, we presented rational design strategies for developing NIR fluorophores with large Stokes shifts and bright emissions. We demonstrated that incorporating a rotary group greatly enlarges the Stokes shifts of fluorophores. We show that the resonance enhancement effect is particularly striking in low-polarity dyes for boosting the second absorption band of the 2PA spectra. This knowledge leads to the systematic development of a new class of NIR fluorophores and biosensors. Fluorophores **1** and **2** possess NIR wavelengths (absorption/emission ≈660/≈740 nm), large Stokes shifts (≈80 nm), excellent photostability, good water solubility, low toxicity, and facile synthesis, making them highly suited for bioimaging and biosensing applications in live cells and animals. Notably, their TP action cross-sections amount to ≈185 GM at 820 nm, which is among the top-notch of organic NIR probes. Our results shed light on the rational molecular engineering of novel NIR fluorophores. We expect that these fluorophores will serve as a useful platform for a broad range of bioimaging and biosensing applications.

Acknowledgements

The authors acknowledge discussions with Professors Xiaobing Zhang and Weihong Tan from Hunan University. This work was supported by the National Natural Science Foundation of China (NSFC Grants 21605046 and 21572190), the Hong Kong Early Career Scheme Grant (No. 21300714) and the National Research Foundation of Singapore (through Singapore-MIT Alliance for Research and Technology).

Conflict of interest

The authors declare no conflict of interest.

Keywords: fluorescence · fluorescent probes · hydrogen sulphide · near-infrared · two-photon

[1] a) R. Weissleder, *Nat. Biotechnol.* **2001**, *19*, 316 – 316; b) H. S. Choi, S. L. Gibbs, J. H. Lee, S. H. Kim, Y. Ashitate, F. Liu, H. Hyun, G. Park, Y. Xie, S. Bae, *Nat. Biotechnol.* **2013**, *31*, 148 – 153.

[2] a) L. Yuan, W. Lin, K. Zheng, L. He, W. Huang, *Chem. Soc. Rev.* **2013**, *42*, 622 – 661; b) Z. Guo, S. Park, J. Yoon, I. Shin, *Chem. Soc. Rev.* **2014**, *43*, 16 – 29.

[3] F. Würthner, T. E. Kaiser, C. R. Saha-Möller, *Angew. Chem. Int. Ed.* **2011**, *50*, 3376 – 3410; *Angew. Chem.* **2011**, *123*, 3436 – 3473.

[4] L. Yuan, W. Lin, Y. Yang, H. Chen, *J. Am. Chem. Soc.* **2012**, *134*, 1200 – 1211.

[5] K. Umezawa, Y. Nakamura, H. Makino, D. Citterio, K. Suzuki, *J. Am. Chem. Soc.* **2008**, *130*, 1550 – 1551.

[6] a) M. Fu, Y. Xiao, X. Qian, D. Zhao, Y. Xu, *Chem. Commun.* **2008**, 1780 – 1782; b) Y. Koide, Y. Urano, K. Hanaoka, W. Piao, M. Kusakabe, N. Saito, T. Terai, T. Okabe, T. Nagano, *J. Am. Chem. Soc.* **2012**, *134*, 5029 – 5031.

[7] H. M. Kim, B. R. Cho, *Chem. Rev.* **2015**, *115*, 5014 – 5055.

[8] a) J. H. Lee, C. S. Lim, Y. S. Tian, J. H. Han, B. R. Cho, *J. Am. Chem. Soc.* **2010**, *132*, 1216 – 1217; b) S. Singha, D. Kim, B. Roy, S. Sambasivan, H. Moon, A. S. Rao, J. Y. Kim, T. Joo, J. W. Park, Y. M. Rhee, T. Wang, K. H. Kim, Y. H. Shin, J. Jung, K. H. Ahn, *Chem. Sci.* **2015**, *6*, 4335 – 4342; c) B. K. Agrawalla, Y. Chandran, W.-H. Phue, S.-C. Lee, Y.-M. Jeong, S. Y. D. Wan, N.-Y. Kang, Y.-T. Chang, *J. Am. Chem. Soc.* **2015**, *137*, 5355 – 5362; d) L. Li, C.-W. Zhang, G. Y. Chen, B. Zhu, C. Chai, Q.-H. Xu, E.-K. Tan, Q. Zhu, K.-L. Lim, S. Q. Yao, *Nat. Commun.* **2014**, *5*, 3276; e) L. Qian, L. Li, S. Q. Yao, *Acc. Chem. Res.* **2016**, *49*, 626 – 634.

[9] M. G. M. Velasco, E. S. Allgeyer, P. Yuan, J. Grutzendler, J. Bewersdorf, *Opt. Lett.* **2015**, *40*, 4915 – 4918.

[10] J. Fu, L. A. Padilha, D. J. Hagan, E. W. Van Stryland, O. V. Przhonska, M. V. Bondar, Y. L. Slominsky, A. D. Kachkovski, *J. Opt. Soc. Am. B* **2007**, *24*, 56 – 66.

[11] a) J. Wang, B. Li, W. Zhao, X. Zhang, X. Luo, M. E. Corkins, S. L. Cole, C. Wang, Y. Xiao, X. Bi, Y. Pang, C. A. McElroy, A. J. Bird, Y. Dong, *ACS Sens.* **2016**, *1*, 882 – 887; b) W. Sun, J. Fan, C. Hu, J. Cao, H. Zhang, X. Xiong, J. Wang, S. Cui, S. Sun, X. Peng, *Chem. Commun.* **2013**, *49*, 3890 – 3892.

[12] a) M. Drobizhev, N. S. Makarov, S. E. Tillo, T. E. Hughes, A. Rebane, *Nat. Methods* **2011**, *8*, 393 – 399; b) M. Drobizhev, N. Makarov, T. Hughes, A. Rebane, *J. Phys. Chem. B* **2007**, *111*, 14051 – 14054.

[13] N. S. Makarov, M. Drobizhev, A. Rebane, *Opt. Express* **2008**, *16*, 4029 – 4047.

[14] X. Liu, Z. Xu, J. M. Cole, *J. Phys. Chem. C* **2013**, *117*, 16584 – 16595.

[15] X. Liu, Q. Qiao, W. Tian, W. Liu, J. Chen, M. J. Lang, Z. Xu, *J. Am. Chem. Soc.* **2016**, *138*, 6960 – 6963.

[16] A. Kanitz, H. Hartmann, P. Czerney, *J. Prakt. Chem./Chem.-Ztg.* **1998**, *340*, 34 – 44.

[17] G. Yang, L. Wu, B. Jiang, W. Yang, J. Qi, K. Cao, Q. Meng, A. K. Mustafa, W. Mu, S. Zhang, *Science* **2008**, *322*, 587 – 590.

[18] A. R. Lippert, E. J. New, C. J. Chang, *J. Am. Chem. Soc.* **2011**, *133*, 10078 – 10080.

Manuscript received: March 26, 2017

Accepted manuscript online: May 8, 2017

Version of record online: June 7, 2017